J|A|C|S
ARTICLES

Published on Web 09/29/2010

Multifunctional Hybrid Organic−Inorganic Catalytic Materials with a Hierarchical System of Well-Defined Micro- and Mesopores

Avelino Corma,* Urbano Díaz,* Teresa García, Germán Sastre, and Alexandra Velty

Instituto de Tecnología Química, UPV-CSIC, Universidad Politécnica de Valencia, Avenida de los Naranjos s/n, E-46022 Valencia, Spain

Received July 22, 2010; E-mail: acorma@itq.upv.es; udiaz@itq.upv.es

Abstract: Novel layered zeolitic organic−inorganic materials (MWW-BTEB) have been synthesized by intercalation and stabilization of arylic silsesquioxane molecules between inorganic zeolitic MWW layers. The organic linkers are conformed by two condensed silyl-arylic groups from disilane molecules, such as 1,4-bis(triethoxysilyl)benzene (BTEB), which react with the external silanol groups of the zeolitic layers. The hybrids contain micropores within the inorganic layers and a well-defined mesoporous system in between the organic linkers. An amination post-treatment introduces basic groups in the organic linkers close to the acid sites present in the structural inorganic counterpart. Through this methodology it has been possible to prepare bifunctional acid−base catalysts where the acid sites are of zeolitic nature located in the inorganic building blocks and the basic sites are part of the organic structure. The resultant materials can act as bifunctional catalysts for performing a two-step cascade reaction that involves the catalytic conversion of benzaldehyde dimethylacetal into benzylidene malononitrile.

1. Introduction

The preparation of multifunctional materials with applications in nanotechnology and catalysis is a matter of much interest.[1−4] In this context, structured porous hybrid materials appear as useful nanosystems where organic and inorganic components interact covalently as building blocks at nanometric scale, imparting the advantages of conventional inorganic oxides (higher thermal, mechanical and structural stability) and organic polymers (specific functionality and high flexibility).[5,6] There are different synthesis methodologies to generate hybrid materials, which go from conventional sol−gel coprecipitation,[7] to more sophisticated coating[8] or self-assembling techniques,[9] the use of layered inorganic precursors being one of the most efficient routes to obtain structured nanohybrids by introducing specific organic molecules into the interlayer space.[10] The versatility of lamellar precursors is confirmed through reported studies on swelling,[11] pillarization[12] or exfoliation/delamination[13,14] preparation procedures.

Layered precursors with ion-exchange capacity allow incorporating a large variety of organic compounds by ion exchange in between the inorganic layers.[15] Traditionally, this method has been widely used with charged inorganic precursors such as clays[16] or anionic clays such as hydrotalcites.[17] In these materials, their tendency to lodge ionic organic molecules such as, for instance, alkylammonium groups and to generate organoclays is used to produce components for industrial polymers.[18] More recently, aminoacids such as proline have been introduced in the interlayer region of montmorillonites, generating interesting enantioselective catalysts for aldolization processes.[19] Rojo et al. have prepared layered hybrid materials using magadiite as silicate precursor and alkylsilanes, such as $(CH_3)_3Si(OEt)$, which act as anchoring agents by covalent interaction of external silanol groups in the silicate layers with alkoxide groups from functionalized monosilanes. This grafting reaction was realized in one direct step without a preswelling process favored by the use of polar solvents.[20] Following this

(1) Sánchez, C. C.; Julián, B.; Belleville, P.; Popall, M. *J. Mater. Chem.* **2005**, *15*, 3559.
(2) Margelefsky, E. L.; Zeidan, R. K.; Davis, M. E. *Chem. Soc. Rev.* **2008**, *37*, 1118.
(3) Boronat, M.; Climent, M. J.; Corma, A.; Iborra, S.; Montón, R.; Sabater, M. J. *Chem.—Eur. J.* **2010**, *16*, 1221.
(4) Climent, M. J.; Corma, A.; Iborra, S.; Mifsud, M. *J. Catal.* **2007**, *247*, 223.
(5) Eddaoudi, M.; Moler, D. B.; Li, H.; Chen, B.; Reineke, T. M.; O'Keeffe, M.; Yaghi, O. M. *Acc. Chem. Res.* **2001**, *34*, 319.
(6) Hoffmann, F.; Cornelius, M.; Morell, J.; Fröba, M. *Angew. Chem., Int. Ed.* **2006**, *45*, 3216.
(7) Corriu, R. J. P.; Mehdi, A.; Reyé, C. *J. Mater. Chem.* **2005**, *15*, 4285.
(8) Nicole, L.; Boissière, C.; Grosso, D.; Quach, A.; Sánchez, C. *J. Mater. Chem.* **2005**, *15*, 3598.
(9) Inagaki, S.; Guan, S.; Fukushima, Y.; Ohsuna, T.; Terasaki, O. *J. Am. Chem. Soc.* **1999**, *121*, 9611.
(10) Ruiz-Hitzky, E.; Darder, M.; Aranda, P. *J. Mater. Chem.* **2005**, *15*, 3650.
(11) Kwon, O. Y.; Shin, H. S.; Choi, S. W. *Chem. Mater.* **2000**, *12*, 1273.
(12) Pinnavaia, T. J.; Ming-Shin, T.; Landau, S. D.; Raythatha, R. *J. Mol. Catal.* **1984**, *27*, 195.
(13) Occelli, M. L. *Stud. Surf. Sci. Catal.* **1988**, *355*, 101.
(14) Corma, A.; Díaz, U.; Dómine, M. E.; Fornés, V. *Angew. Chem., Int. Ed.* **2000**, *39*, 1499.
(15) Sprung, R.; Davis, M. E.; Kauffman, J. S.; Dybowski, C. *Ind. Eng. Chem. Res.* **1990**, *29*, 213.
(16) Tamura, K.; Nakazawa, M. *Clays Clay Miner.* **1996**, *44*, 501.
(17) Li, L.; Ma, R.; Ebina, Y.; Iyi, N.; Sasaki, T. *Chem. Mater.* **2005**, *17*, 4386.
(18) Ogawa, M.; Kuroda, K. *Bull. Chem. Soc. Jpn.* **1997**, *70*, 2593.
(19) Srivastava, V.; Gaubert, K.; Pucheault, M.; Vaultier, M. *ChemCatChem* **2009**, *1*, 94.
(20) Ruiz-Hitzky, E.; Rojo, J. M. *Nature* **1980**, *287*, 28.

work, ilerite (also called RUB-18) and octosilicate have been employed as precursors to produce different two-dimensional (2D) or 3D hybrid porous materials by intercalation of chlorosilanes ($ROSiCl_3$) or bridged silsesquioxanes ($((R'O)_3SiRSi(OR')_3$), containing benzene or biphenyl groups as pillaring agents.[21−23] However, the layered materials obtained from silicates exhibit frequently an irregular porosity, a nonhomogeneous organic pillars distribution and, frequently, an undesirable polymerization between silsesquioxane molecules. These disadvantages, together with the relatively poor structural order and crystallinity showed by the layered silicates,[24] can be an inconvenient for the potential application of these materials. An alternative route to avoid the above problems can be to use highly ordered, crystalline, stable layered zeolite precursors as building units to generate homogeneous layered hybrid materials by intercalation of suitable silsesquioxanes in the interlayer space. The more organized structure of the zeolitic layers could facilitate the preparation of hybrid materials with the high mechanical and thermal stability characteristic of zeolites, combined with the high accessibility achieved within the interlayer space due to the presence of the organic spacers, which can also be functionalized. The layered precursor of MWW zeolite[25] has been used to generate silica-pillared (MCM-36)[26,27] and delaminated (ITQ-2)[28] materials. Recently, Tatsumi et al. have introduced, between the layers, one atom of silicon to obtain new interlayer expanded zeolites (IEZ).[29] Moreover, studies related to the grafting of titanocene groups on individual MWW layers[30] or the encapsulation of photoluminescent molecules into the semicups of ITQ-2[31] show the capacity of this MWW-based layered materials to generate hybrid materials.

Here, we present novel, layered, hybrid zeolitic materials (MWW-BTEB) prepared by pillaring the MWW precursors with bridged silsesquioxanes, also called disilanes, this being the first time, to our knowledge, that this has been carried out with zeolitic building blocks. More specifically, 1,4-bis(triethoxysilyl)benzene (BTEB) is employed as the organic agent that interacts with the layered precursor of MWW zeolite. The presence of stabilized organic fragments in the interlayer space, bonded covalently to MWW individual layers, generates structured hybrid materials as confirmed by a variety of characterization techniques such as elemental and textural analyses, XRD, NMR, IR, TEM and molecular modeling. Postsynthesis treatments of the zeolitic hybrids have allowed the functionalization of the organic counterpart with basic amino groups which, together with the acid sites generated by the presence of tetrahedrally coordinated framework aluminiums in the individual MWW layers, result in bifunctional acid−base catalysts. Their potential has been shown for the one-pot synthesis of benzylidene malononitrile from malononitrile and benzaldehyde dimethylacetal. The process involves the hydrolysis of the acetal catalyzed by the Brønsted acid sites present in the inorganic building blocks, followed by a Knoevenagel condensation reaction catalyzed by the basic sites located in the organic fragments which form the mesoporous gallery.

2. Experimental Section

2.1. Synthesis. 2.1.1. Synthesis of the MWW Layered Zeolitic Precursor (MWW-P). The synthesis of MWW zeolitic precursors was carried out following the procedure described in ref 32. Typically, 0.46 g of sodium aluminate (56%Al_2O_3, 37%Na_2O, Carlo Erba) and 1.62 g of sodium hydroxide (98%, Aldrich) were dissolved in 203.90 g of distilled water, after which 12.70 g of hexamethylenimine (HMI, 98%, Aldrich) and 15.72 g silica (Aerosil 200, Degussa) were added consecutively. The mixture was stirred vigorously for 30 min at room temperature, producing a gel with a silicon to aluminum atomic ratio of 50 (corresponding to a silica to alumina molar ratio of 100). The crystallization of the lamellar precursor was done at 408 K during 11 days in a stirred PTFE-lined stainless-steel autoclave under autogenous pressure. The crystalline product was filtered and washed with distilled water until pH < 9. The material filtered and dried at 333 K during 12 h shows the XRD characteristic of the MWW laminar precursor.

2.1.2. Swelling of MWW Layered Zeolitic Precursor (MWW-CTMA). In order to prepare the swollen MWW material, 10 g of the lamellar precursor was dispersed in 40 g of H_2O Milli-Q, and 200 g of a cetyltrimethylammonium hydroxide solution (CTMA, 25 wt %, 50% exchanged Br^-/OH^-) was added, the final pH being ∼12.5. The resultant mixture was refluxed at 353 K, stirring vigorously for 16 h in order to facilitate the swelling of the layers of the inorganic precursor material. At this point, the swollen material was recovered by centrifugation, washed with distilled water, and dried at 333 K for 12 h.

2.1.3. Intercalation of Swollen MWW Precursor with Aryl-Bridged Silsesquioxanes (MWW-CTMA-BTEB). The swollen MWW zeolitic precursor (0.5 g) was vigorously stirred with a dioxane solution (50 mL) of pillaring agents such as 1,4-bis(triethoxysilyl)benzene (BTEB, 0.5 g, ABCR) for 2 days at 353 K. This process was carried out under inert atmosphere (N_2). The white solid obtained was recovered from the suspension by filtration, first with dioxane and second with ethanol. The compounds were then air-dried for 5 days at room temperature.

2.1.4. Synthesis of the Organic−Inorganic Zeolitic Hybrid Material (MWW-BTEB). To remove the CTMA employed as swollen agents, an acid extraction process was performed in two consecutive steps. First, the organic−inorganic hybrid compounds (1.0 g) were suspended and refluxed in 50 mL of 0.05 M H_2SO_4 ethanol solution for 1 h at 343 K. The solid obtained was filtered and washed with ethanol and air-dried for 8 h at 333 K. Second, the fine white powder recovered was suspended in 50 mL of 0.15 M HCl ethanol/*n*-heptane solution (1/1, v/v) for 16 h at 363 K. The intercalated final products were recovered after filtration with ethanol/*n*-heptane (1/1, v/v) solution and air-dried at 333 K overnight.

For comparison, the removing of swollen agents was also carried out by calcination at 400 °C in air during 8 h (MWW-BTEB-CAL).

2.1.5. Incorporation of Amino (−NH_2) Groups in the Zeolitic Hybrid Materials (MWW-BTEB-NH_2). To incorporate amino groups on the bridged benzene groups in the interlayer space, 0.5 g of MWW-BTEB was suspended in 15.2 g of H_2SO_4 (98%, Aldrich) and 3.47 g of HNO_3 (65%, Panreac) for 3 days at room temperature. The acid mixture was previously prepared, and it was slowly added over the solid. After this, cold distilled water (300 mL) was added,

(21) Shimojima, A.; Mochizuki, D.; Kuroda, K. *Chem. Mater.* **2001**, *13*, 3603.
(22) Ishii, R.; Shinohara, Y. *J. Mater. Chem.* **2005**, *15*, 551.
(23) Ishii, R.; Ikeda, T.; Itoh, T.; Ebina, T.; Yokoyama, T.; Hanaoka, T.; Mizukami, F. *J. Mater. Chem.* **2006**, *16*, 4035.
(24) Beneke, K.; Lagaly, G. *Am. Mineral.* **1983**, *68*, 818.
(25) Leonowicz, M. E.; Lawton, J. A.; Lawton, S. L.; Rubin, M. K. *Science* **1994**, *264*, 1910.
(26) Roth, W. J.; Kresge, C. T.; Vartuli, J. C.; Leonowicz, M. E.; Fung, A. S.; McCullen, S. B. *Stud. Surf. Sci. Catal.* **1995**, *94*, 301.
(27) He, Y. J.; Nivarthy, G. S.; Eder, F.; Seshan, K.; Lercher, J. A. *Microporous Mesoporous Mater.* **1998**, *25*, 207.
(28) Corma, A.; Fornés, V.; Pergher, S. B. C.; Maesen, Th. L.; Buglass, J. G. *Nature* **1998**, *396*, 353.
(29) Wu, P.; Ruan, J.; Wang, L.; Wu, L.; Wang, Y.; Liu, Y.; Fan, W.; He, M.; Terasaki, O.; Tatsumi, T. *J. Am. Chem. Soc.* **2008**, *130*, 8178.
(30) Corma, A.; Díaz, U.; Fornés, V.; Jordá, J. L.; Dómine, M.; Rey, F. *Chem. Commun.* **1999**, 779.
(31) Corma, A.; Díaz, U.; Ferrer, B.; Fornés, V.; Galletero, M. S.; García, H. *Chem. Mater.* **2004**, *16*, 1170.
(32) Corma, A.; Corell, C.; Pérez-Pariente, J. *Zeolites* **1995**, *15*, 2.

and the formed solution was stirred for 4 h at room temperature. The pale-yellow solid obtained was recovered by filtration and washed with abundant distilled water and air-dried at 333 K for 8 h. Next, the dried solid was supended in a previously prepared solution of 15 mL of HCl (37%, Aldrich) and 1.59 g of $SnCl_2$ (98%, Aldrich), and the stirring was maintained for another 3 days at room temperature. After this, 300 mL of distilled water was added into the solution, and the stirring was continued for another 4 h. The yellow sample was recovered by filtration and washed with distilled water (100 mL) and ethanol (100 mL). Finally, the solid with amino groups was air-dried at 333 K for 8 h.[33]

2.2. One-Pot Catalytic Reaction. Before the catalytic test, the HYB-BTEB-NH_2 material was pretreated with buffer aqueous solution of NH_4Cl/NH_4OH (0.1 wt %, pH = 10−11) by 1 h stirring at room temperature, filtered, washed with ethanol and dried at 473 K to neutralize the protonated amino groups formed during the amination process.

Next, a mixture of benzaldehyde dimethylacetal (5.45 mmol), malononitrile (5.24 mmol), H_2O (30 μL or 0.33 mol %) and the layered hybrid catalyst (50 mg or 0.1 mol % of amino) were kept at 353 K under magnetic stirring. The reaction mixture was then stirred under a nitrogen atmosphere, and the kinetic was followed by taking samples within time periods of 0.25−12 h. The products were analyzed by GC and GC−MS equipped with an Equity-5 column (30 m × 0.25 m× 0.25 μm) and a FID as detector. For catalyst recycling studies, the used catalyst was filtered and washed with ethyl acetate. The recovered catalyst was used for a new run, and the process was repeated for successive runs.

2.3. Characterization Techniques. XRD analysis was carried out with a Philips X'PERT diffractometer equipped with a proportional detector and a secondary graphite monochromator. Data were collected stepwise over the $2° \leq 2\theta \leq 40°$ angular region, with steps of 0.02° 2θ, 20-s/step accumulation time and Cu Kα (λ = 1.54178 Å) radiation. Transmission electron microscopy (TEM) micrographs were obtained with a JEOL 1200X electron microscope operating at 120 keV. The samples were prepared directly by dispersing the powders onto carbon copper grids. C, N, S and H contents were determined with a Carlo Erba 1106 elemental analyzer, while Al contents were obtained by means of atomic absorption spectroscopy (Spectra AA 10 Plus, Varian). IR spectra were obtained in a Nicolet 710 spectrometer (4 cm^{-1} resolution) using a conventional greaseless cell. Wafers of 10 mg cm^{-2} were outgassed at 100 °C overnight.

Nitrogen and argon adsorption isotherms were measured at 77 and 87.3 K, respectively, with a Micromeritics ASAP 2010 volumetric adsorption analyzer. Before the measurements, the samples were outgassed for 12 h at 100 °C. The BET specific surface area[34] was calculated from the nitrogen adsorption data in the relative pressure range from 0.04 to 0.2. The total pore volume[35] was obtained from the amount of N_2 adsorbed at a relative pressure of about 0.99. External surface area and micropore volume were estimated using the *t*-plot method in the *t* range from 3.5 to 5. The pore diameter and the pore size distribution were performed using the Barret−Joyner−Halenda (BJH) method[36] on the adsorption branch of the nitrogen isotherms. Horvath−Kawazoe method was applied to estimate the microporous distribution from argon isotherms.

Solid-state MAS NMR spectra were recorded at room temperature under magic angle spinning (MAS) in a Bruker AV-400 spectrometer. The single pulse ^{29}Si spectra were acquired at 79.5 MHz with a 7-mm Bruker BL-7 probe using pulses of 3.5 μs corresponding to a flip angle of 3/4 π radians, and a recycle delay of 240 s. ^{27}Al spectra were obtained at 104.2 MHz using a 4-mm Bruker BL-4 probe. Pulses of 0.5 μs to flip the magnetization $\pi/20$ rad, and a recycle delay of 2 s were used. The ^1H to ^{13}C cross-polarization (CP) spectra were acquired by using a 90° pulse for ^1H of 5 μs, a contact time of 5 ms, and a recycle of 3 ms. The ^{13}C spectra were recorded with a 7 mm Bruker BL-7 probe and at a sample spinning rate of 5 kHz. ^{13}C, ^{29}Si and ^{27}Al were referred to adamantine, tetramethylsilane and an aqueous solution of $Al(NO_3)_3$, respectively.

3. Results and Discussion

3.1. Synthesis and Characterization. The preparation of hybrid organic−inorganic materials (MWW-BTEB) with layered precursors of the MWW zeolite and intercalated aryl-bridged silsesquioxane molecules in the interlayer space was performed after the swelling and intercalation of the layered precursors with CTMA and BTEB, respectively. The organic linkers are covalently bonded to the surface of the zeolitic layers by reaction of terminal alkoxide groups from disilanes with silanol groups from the inorganic layers (see Scheme 1). The swelling agents were recovered by acid extraction and the procedure employed to obtain the MWW-BTEB material is presented in Scheme 1a.

The effective intercalation of silyl-aryl groups into the interlayer space of MWW precursors was confirmed by XRD patterns shown in Figure 1. Thus, the diffractogram of MWW-P zeolitic precursor (Figure 1a) exhibits the characteristic 00*l* bands of MWW materials at 27.1 Å and 13.6 Å, assigned to (001) and (002) reflections, respectively, confirming that the inorganic layers are ordered perpendicularly to the *c*-axis. Taking into account the presence of the organic directing agent (HMI) and water molecules between the MWW layers in the zeolitic precursor and observing that the basal spacing is ∼27 Å, it is possible to confirm that the thickness of each individual layer is ∼25 Å. After the swelling process, the basal distance increases to 36.0 Å due to the effective incorporation of CTMA molecules into the interlayer space (Figure 1b). Next, when the intercalation process was carried out with BTEB, the basal space was increased to 40.1 Å in the final layered hybrid material (Figure 1d). Considering the thickness (25 Å) of MWW layers, the space occupied by the aryl-bridged linker from silsesquioxanes corresponds to 15.1 Å, which is close to the molecular length of the two condensed BTEB molecules acting as pillars (Figure 2). This confirms that the starting disilanes, each containing two condensed silyl-benzene groups, were successfully intercalated into the interlayer space perpendicularly to MWW zeolitic layer (see schematic model in Scheme 1b). The diffraction pattern of the hybrid material before acid extraction (Figure 1c) shows two peaks at 44.5 Å and 37.0 Å, indicating that the interlayer space is not uniform due to the simultaneous presence of CTMA and BTEB molecules into the interlayer space. The unhomogeneity disappears when the swelling CTMA molecules were removed and effective covalent bonds were established between BTEB and the silanols of the MWW layers.

When a postsynthesis process was carried out to incorporate amino groups on the arylic fragments (MWW-BTEB-NH_2), the diffraction pattern of the sample obtained (Figure 1e) is similar to that obtained after acid extraction (MWW-BTEB), showing that the amination reaction does not result in any significant modification of the zeolitic hybrid material. It is important to remark that, in all diffractograms, it is possible to observe, invariably, the band at ∼12.1 Å assigned to *1*00 reflection, confirming that the structural integrity of each MWW layer was

(33) Ohashi, M.; Kapoor, M. P.; Inagaki, S. *Chem. Commun.* **2008**, 841.
(34) Gregg, S. J.; Sing, K. S. W. *Adsorption, Surface Area and Porosity*; Academic Press: London, 1982.
(35) Sing, K. S. W.; Everett, D. H.; Haul, R. A. W.; Moscou, L.; Pierotti, R. A.; Rouquerol, J.; Siemieniewska, T. *Pure Appl. Chem.* **1985**, *57*, 603.
(36) Barrett, E. P.; Joyner, L. G.; Halenda, P. P. *J. Am. Chem. Soc.* **1951**, *73*, 373.

Scheme 1. Artistic Representation of (a) Methodology Employed to Obtain Pillared Hybrid Zeolitic Materials from MWW Precursors and (b) Layered Hybrid Material Obtained by Pillaring with BTEB Silsesquioxane Molecules (MWW-BTEB)

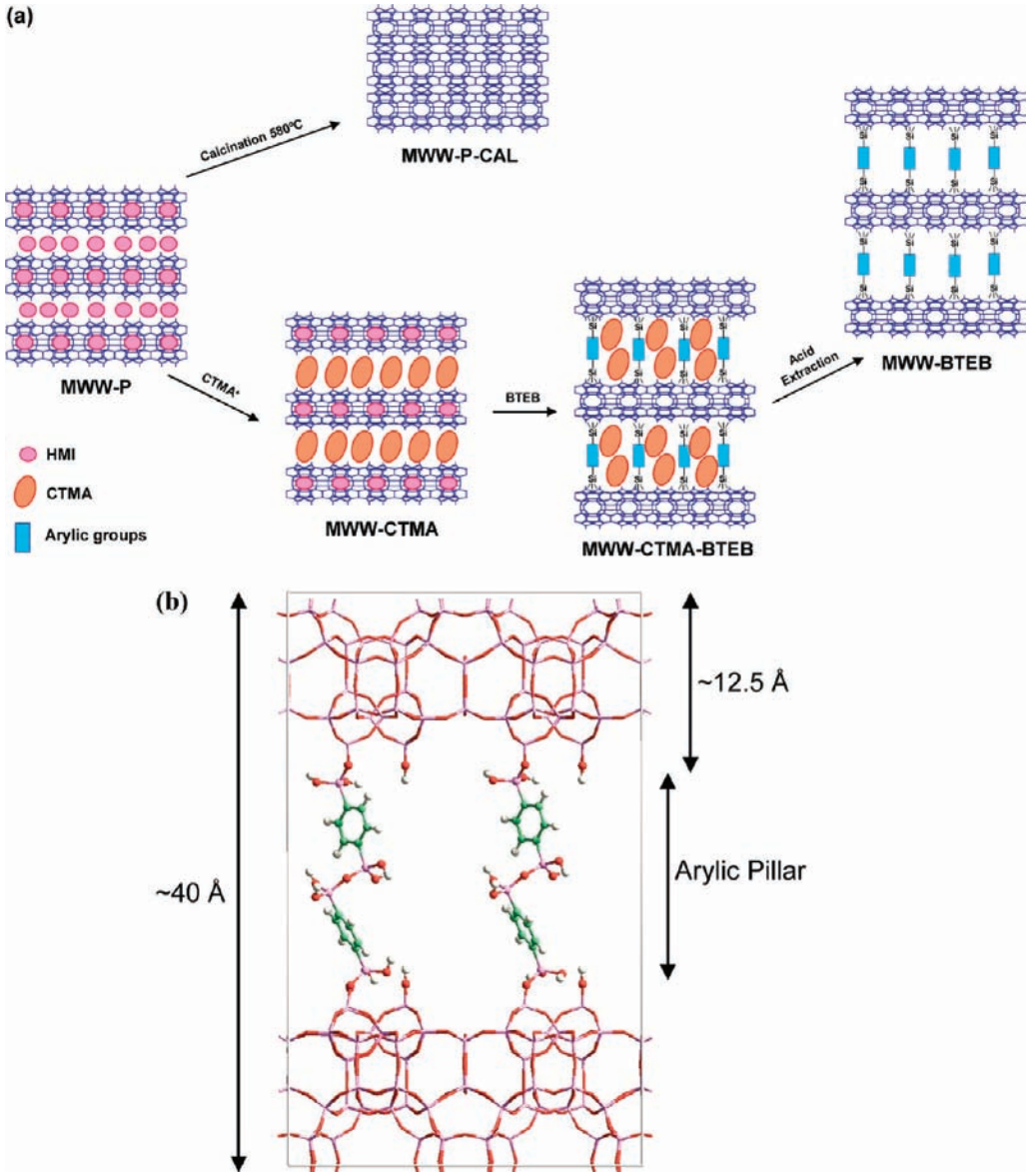

preserved during the intercalation and amination processes. The hybrid material remains stable up to 400 °C. At higher calcinations temperatures, it is possible to observe the absence of low angle diffraction peaks characteristic of the pillared materials (Figure 1f), due to partial removal and decomposition of the arylic pillars, which results in the collapse of the material.

Transmision electron microscopy (TEM) was used to visualize the lamellar morphology of the MWW zeolitic precursors and the layered hybrid materials generated after intercalation with BTEB bridged silsesquioxane molecules (Figure 3). The starting MWW-P precursor appears as a highly crystalline conventional layered material with an ordered lamellar distribution of the different sheets which form each individual crystal (Figure 3a). More specifically, the crystals present a thickness that fluctuates between 150 and 200 nm that corresponds to the presence of approximately 60−80 individual MWW layers which are perpendicularly packed and oriented to the *c* axis (Figure 3b). After the intercalation process, the morphology of the extracted MWW-BTEB materials has been substantially modified (Figure 3c). The hybrid materials present a layered distribution with lower order compared with the MWW precursor, being the crystals conformed by a reduced number of piled MWW layers (between 5 to 8 individual sheets), as can be observed in Figure 3d. In the inset shown in this photograph, it is possible to appreciate the interlayer space between two contiguous layers perpendicularly placed to the *c* axis. The measured value corresponds to approximately 38−40 Å, which is in full agreement with the basal distance estimated from XRD for the hybrid intercalated materials. This fact corroborates that organic pillars of ∼15 Å, conformed by two condensed benzene groups (Scheme 1b), are intercalated into the interlayer zeolitic space.

The potential incorporation of organic fragments in the layered MWW zeolitic silica precursor was also followed by means of CHN elemental analyses. The estimated weight of organic species present in the swollen and BTEB intercalated materials are shown in Table 1. The organic content obtained in each sample could be a clear indication of the effective incorporation of swollen and/or pillaring agents in the interlayer space of zeolitic precursor. In the case of the starting zeolitic

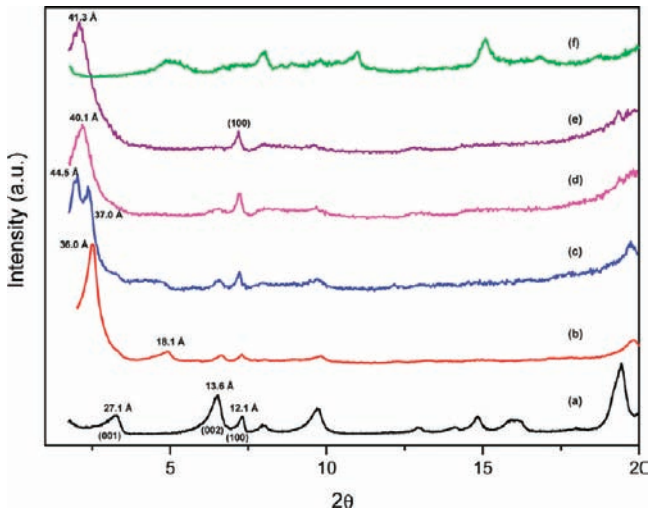

Figure 1. Powder X-ray diffraction patterns of (a) MWW-P, (b) MWW-CTMA, (c) MWW-CTMA-BTEB, (d) MWW-BTEB, (e) MWW-BTEB-NH_2 and (f) MWW-BTEB-CAL.

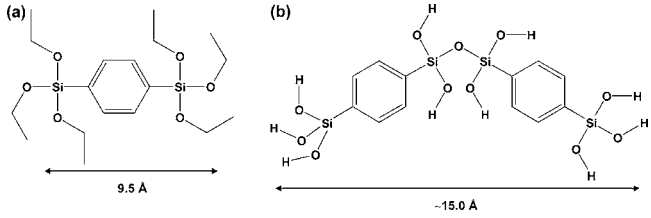

Figure 2. Bridged silsesquioxanes: (a) 1,4-bis(triethoxysilyl)benzene (BTEB) and (b) arylic pillaring agents derived of BTEB.

precursor (MWW) the C/N experimental molar ratio is 6.6, which is close to the theoretical ratio calculated (C/N = 6.0) for the organic structure agent (HMI) used to synthesize the zeolite precursor. After the swelling process, the resultant MWW-CTMA shows a remarkable increase in carbon content (20.1% in the swollen material), confirming that CTMA molecules could be present in the interlayer space. When the intercalation process is carried out with BTEB silsesquioxanes (MWW-CTMA-BTEB), the carbon content is further increased (26.3% wt) probably due to the presence of aryl groups between the MWW layers together with CTMA molecules. The analysis of extracted sample (MWW-BTEB) clearly shows that the swollen agents were removed by the acid extraction. Considering the carbon content of the intercalated sample, it is possible to conclude from elemental analyses that approximately 10 wt % of the layered zeolitic hybrid corresponds to arylic groups incorporated into the samples (Table 1).

The incorporation of amino groups, during the postsynthesis amination, was confirmed by elemental analysis. Indeed, the nitrogen content is increased up to 1.3 wt %, being the experimental C/N molar ratio of 6.7. This result indicates that some interlayered benzene groups could be functionalized with at least one amino group. It has to be remarked that the acid procedure used for the amination process was responsible for a partial dealumination of the solids since the experimental Si/Al molar ratio was increased up to 80 in the final MWW-BTEB-NH_2 material (Table 1).

3.1.1. Spectroscopic Characterization. It is possible to confirm by IR spectroscopy, the presence and integrity of arylic species between the layered zeolitic precursors in the hybrid MWW-BTEB material (Figure 4). The IR spectrum of the MWW-BTEB hybrid sample exhibits, in comparison with the MWW calcined precursor, additional bands at ∼1400, ∼1600, 3020, and 3060 cm^{-1} associated to the silicon-phenyl asymmetric stretching vibrations, indicating the presence of aromatic groups (spectra a and b of Figure 4). Small bands were also observed at 2860 and 2980 cm^{-1} which can be due to the presence of arylic groups and residual hydrocarbon fragments from the swelling (CTMA) or the structural directing agent (HMI) which remain after the acid extraction. Moreover, the conventional peak assigned to silanol groups (3730 cm^{-1} in Figure 4a) present in the calcined zeolitic precursor is partially shifted to ∼3500 cm^{-1} (Figure 4b) when the aryl groups are incorporated into the zeolitic material, being this probably due to the proximity between external layered Si−OH and intercalated silyl-aromatic groups. The additional broad band around 3620 cm^{-1} is due to the interaction of water molecules with the surface silanol groups.[37]

The IR spectrum of the solid obtained after the amination process (Figure 4c) shows new additional bands at 1540 and 1630 cm^{-1} assigned to δ-(NH_2) bending vibrations together with one characteristic band at 3400 cm^{-1} due to ν-(NH_2) stretching vibration, confirming that amino groups are effectively incorporated to the arylic species. The presence of the bands assigned to benzene groups, in the IR spectrum of the MWW-BTEB-NH_2 sample, shows that the integrity of arylic species is preserved during amination step. In conclusion, the IR spectroscopy verifies unambiguously the presence of the aryl and amino-aryl species into the zeolitic hybrid materials.

^{13}C CP/MAS NMR chemical shifts shown in Figure 5 confirm the effectiveness of the intercalation process and the integrity of the arylic groups introduced into the interlayer space of MWW zeolitic precursors. In the cases of MWW-P, MWW-CTMA and MWW-BTEB materials, it is possible to see the bands assigned to carbon atoms from structural directing agents (HMI), swelling agents (CTMA) and BTEB bridged silsesquioxane molecules (see spectra a, b, and c of Figure 5, respectively), including the carbon atoms directly bonded to Si. This observation corroborates that aryl bridged fragments remain intact as in the initial BTEB disilane precursors. The strong reduction of the bands associated to CTMA swelling molecules confirms the effectiveness of the acid extraction process. The postfunctionalization of derived benzene fragments with amino groups is confirmed by NMR (Figure 5d) since the band assigned to aromatic carbons is divided into three signals, being the band at ∼150 ppm associated to the amino covalently bonded to arylic groups.[38]

From the ^{13}C NMR chemical shifts, we are able to conclude that organic units preserve their integrity during the intercalation step. Now, to corroborate that the organic bridges not only remain intact but are also incorporated covalently into the interlayer space as organic pillars, the ^{29}Si NMR analysis was performed. Figure 6 shows ^{29}Si BD/MAS NMR chemical shifts of the different materials obtained during the preparation of hybrid layered materials. The spectrum of the MWW zeolitic precursor (MWW-P) (Figure 6a) shows the signals corresponding to Q^2 ($Si(OH)_2(OSi)_2$), Q^3 ($Si(OH)(OSi)_3$) and Q^4 ($Si(OSi)_4$) units at −95, −100, and −110 to −120 ppm, respectively, being also possible to observe the band at −105 ppm corresponding

(37) Sauer, J.; Ugliengo, P.; Garrone, E.; Saunders, V. R. *Chem. Rev.* **1994**, *94*, 2095.
(38) Pretsch, E.; Clerc, T.; Seibl, J.; Simon, W. *Structural Elucidation of Organic Compounds Using Spectroscopic Methods*; Springer Verlag: Berlin - Heidelberg - New York, 1976.

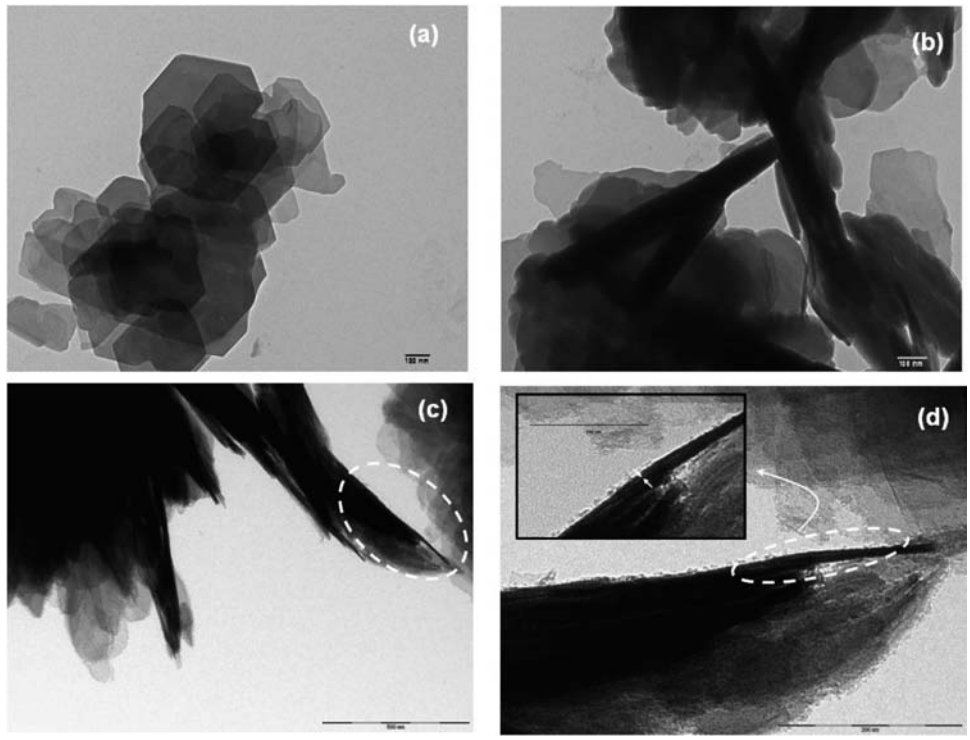

Figure 3. TEM micrographs: (a) and (b) MWW-P, (c) and (d) MWW-BTEB.

Table 1. Organic Incorporation into the Hybrid Type-MWW Materials Estimated by Elemental Analysis; Aluminium Content Is Also Shown from Chemical Analysis

sample	C/%	N/%	H/%	C/N	organic content (EA)[a]/%	Si/Al[b]
MWW-P	9.6	1.7	2.1	6.6	13.4	47
MWW-CTMA	20.1	1.7	4.1	14.2	25.9	52
MWW-CTMA-BTEB	26.3	1.5	4.2	20.5	32.0	51
MWW-BTEB	12.2	0.2	2.2	71.2	14.6	55
MWW-BTEB-NH_2	7.4	1.3	2.1	6.7	10.8	81
MWW-BTEB-CAL	1.8	0.2	0.9	12.6	2.9	59

[a] EA: Elemental analysis. [b] Chemical analysis.

to Si(1Al) due to $Si(OSi)_3(OAl)$ species. When the pillarization step is carried out, the spectrum of MWW-BTEB samples (Figure 6b) shows bands in the −60 to −80 ppm which correspond to T-type silicon species having a Si−C bond from bridged disilanes intercalated into the interlayer space. More specifically, it is possible to observe three bands assigned to T^1 ($C-Si(OH)_2(OSi)$), T^2 ($C-Si(OH)(OSi)_2$) and T^3 ($C-Si(OSi)_3$) (see Figure 6). The variation in the intensities observed for the Q^4 silicon atoms when comparing the spectra of MWW-P and MWW-BTEB, could be due to the generation of new Q^4 silicon atoms in the hybrid from surface Q^3 silanol groups present in the zeolitic precursor after the intercalation process. Moreover, the existence of T^1 and T^2 silicon atoms in the pillared samples could indicate that during the hydrolysis and condensation with the surface silanol groups present in the MWW layers, not all terminal alkoxide groups from BTEB molecules are involved in this process. These silicon atoms could also be assigned to Si−OH groups contained into the interlayer pillars generated during the condensation between two BTEB silsesquioxane molecules.

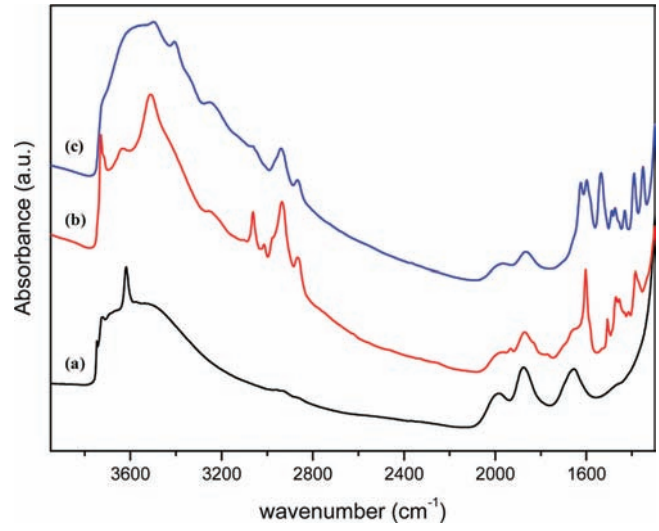

Figure 4. IR spectra of (a) MWW-P-CAL, (b) MWW-BTEB and (c) MWW-BTEB- NH_2.

The amination post-treatment does not imply any substantial modification of the organic fragments inserted into the interlayer space since the same T-type species are observed. However, the acid procedure used for the amination process probably results in a certain crystallinity loss of the MWW layers, as it can be deduced from the poor resolution of the Q-type silicon bands (Figure 6c). Nevertheless, this observation can also be associated to a partial dealumination occurring during the acid treatment (Table 1).

Another confirmation of the effective incorporation of organic linkers into the MWW precursors comes from ^{29}Si NMR of the starting BTEB bridged silsesquioxanes shown in Figure 6d. The pure disilane exhibits only one peak characteristic of silicon atoms centered at −59 ppm. After the covalent insertion of arylic groups in between the MWW layers, the signal assigned to

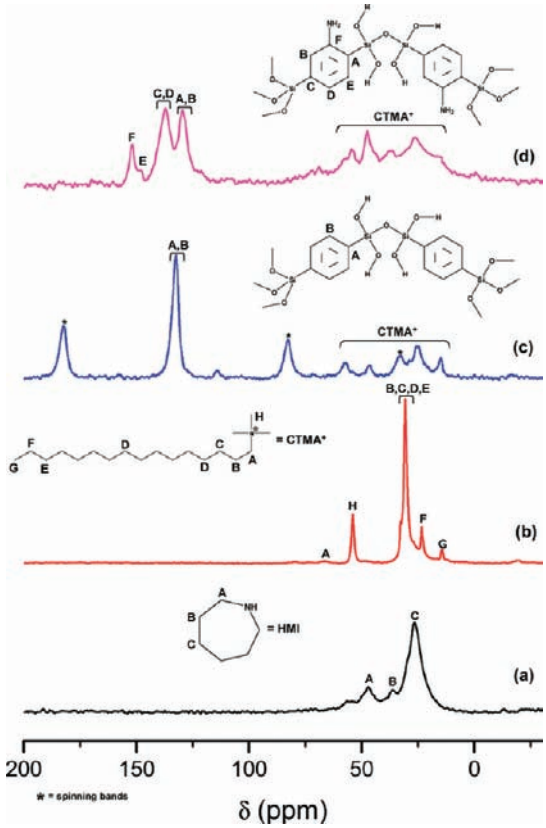

Figure 5. ^{13}C CP/MAS NMR spectra of different layered hybrid zeolitic materials, showing the assignment of the bands with the carbon atoms contained into the solids: (a) MWW-P, (b) MWW-CTMA, (c) MWW-BTEB and (d) MWW-BTEB-NH_2.

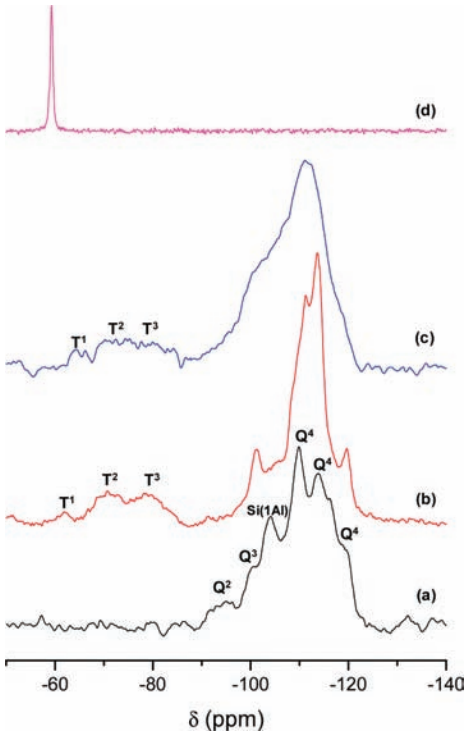

Figure 6. ^{29}Si BD/MAS NMR spectra of different layered hybrid zeolitic materials, showing the assignment of T- and Q-type silicon atoms: (a) MWW-P, (b) MWW-BTEB, (c) MWW-BTEB-NH_2 and (d) pure 1,4-bis(triethoxysilyl)benzene.

silicon atoms bonded to carbon units is shifted from −60 ppm to −80 ppm (Figure 6), something which corroborates the integration of organic linkers within the interlayer space.

The integrated ratios $(Q^2 + Q^3)/Q$ obtained for MWW zeolitic precursor and for extracted MWW-BTEB pillared material, can be useful to corroborate that terminal reactive alkoxide groups from silsesquioxanes are hydrolyzed onto external silanols at the surface of MWW layers. In the case of zeolitic precursor, this ratio is 0.41, decreasing after the pillarization process to 0.25. This result shows that approximately 60% of initial silanol groups were involved in the covalent insertion of disilane groups between contiguous inorganic layers. Moreover, the integration of the signals (T and Q) present in the ^{29}Si BD/MAS NMR chemical shifts (Figure 6) allows calculating the ratio $T/(Q + T)$ and giving one estimation of the number of functionalized silicon atoms in the layered hybrid materials. The values obtained show that approximately 21% of the silicon atoms are functionalized by arylic species in the final MWW-BTEB sample, this value being close to the value calculated from elemental analyses (23%).

The presence of framework aluminum in the MWW hybrid materials is clearly confirmed by ^{27}Al MAS/NMR chemical shifts (Figure S1, Supporting Information), since the hybrid samples with silyl-arylic groups, before and after the amination, only exhibit one broad peak focused at ∼56 ppm that can be assigned to tetrahedral aluminum. A band at ∼0 ppm, which can be assigned to extraframework aluminum, was not observed. The presence of Al^{IV} in the inorganic layer of the hybrid material supports the presence of bridged hydroxyls and, consequently, the existence of zeolitic acidic groups. Then, the presence of Brønsted acid in the inorganic layers and basic groups in the interlayer gallery indicate the possibility to prepare well-defined bifunctional hybrid organic−inorganic materials by the here described methodology.

3.1.2. Textural Properties. Table 2 shows the textural properties of the different materials obtained. The results confirm that the introduction of silyl-aryl groups into the interlayer space implies significant modifications on the surface and porosity of the resulting materials. Thus, the BET surface area of the calcined MWW precursor (MWW-P-CAL) is 408 $m^2\ g^{-1}$, while when the intercalation process is carried out (MWW-BTEB), the BET surface area increases up to 539 $m^2\ g^{-1}$, with 70% corresponding to meso and external surface area due to the highest accessibility achieved. The BJH volume obtained also indicates an important enhancement of the mesoporous surface area in the hybrid materials after the intercalation process (0.234 $cm^3\ g^{-1}$). The hybrid organic−inorganic prepared after the amination (MWW-BTEB-NH_2) exhibits a surface area distribution and pore volume similar to the extracted pillared material (MWW-BTEB), indicating that the incorporation of amino groups onto derived aryl groups have not substantially modified the mesoporous system (Table 2). When the extraction of swelling agents is performed by calcination (MWW-BTEB-CAL), the aryl groups are partially decomposed, favoring the collapse between the MWW layers. When this occurs, the surface area and porous volume are similar to those of conventional microporous MWW calcined materials.

The N_2 adsorption isotherm of the calcined zeolitic precursor (Figure 7) is similar to a conventional type I isotherms characteristic of microporous materials with little mesoporosity. On the other hand, the extracted MWW-BTEB sample shows an isotherm with a shift of the inflection point toward higher relative pressures, indicating that the mesoporous contribution

Table 2. Mean Textural Properties of Hybrid Porous Organic−Inorganic Materials

sample	S_{BET} (m^2 g^{-1})	S_{micro} (m^2 g^{-1})	S_{ext}[a] (m^2 g^{-1})	V_{tot} (cm^3 g^{-1})	V_{micro} (cm^3 g^{-1})	V_{BJH} (cm^3 g^{-1})	BJH mean pore diameter (Å)
MWW-P-CAL	408	325	83	0.512	0.170	0.078	micropore
MWW-BTEB	539	151	388	0.640	0.070	0.234	54
MWW-BTEB-NH_2	556	112	444	0.685	0.054	0.267	42
MWW-BTEB-CAL	386	315	71	0.413	0.150	0.080	micropore

[a] $S_{ext} = (S_{BET} - S_{micro})$.

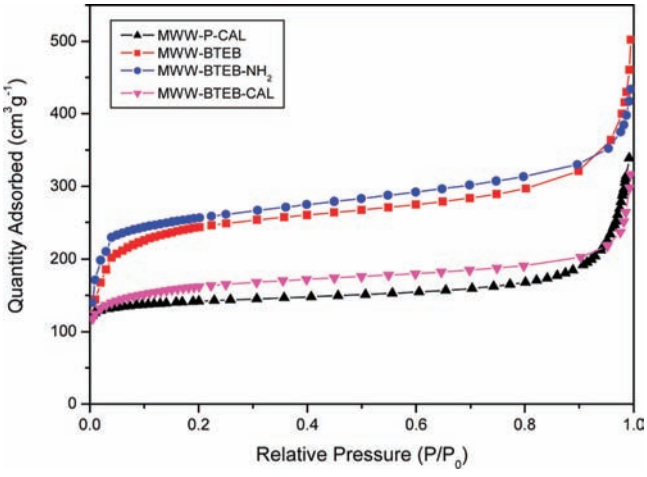

Figure 7. Nitrogen adsorption isotherms of different zeolitic type-MWW materials.

and the pore diameter (∼54 Å) is larger than for nonpillared materials. Indeed, the isotherm for MWW-BTEB shows an increase of the adsorption at p/p_o between 0.3 and 0.4, which corresponds to mesoporosity, being this absent in the calcined MWW precursor. Additional confirmation can be obtained from the Ar isotherms (Figure S2, Supporting Information), which clearly show that all samples have a system of pores which starts to fill up at $p/p_o \approx 5 \times 10^{-6}$. A second inflection point in the isotherm at $p/p_o \approx 5 \times 10^{-3}$ is present in the calcined MWW zeolitic precursors but it is absent in the hybrid pillared materials. Since the first inflection corresponds to the filling of the 10 MR micropores while the second is assigned to the filling of the 12 MR pores within the MWW structure, it is possible to conclude that the 12 MR supercages formed in the MWW zeolite do not exist in the intercalated hybrid materials (Figure 7 and S2, Supporting Information). When the calcination process is performed at 400 °C, the shape of the N_2 isotherms is similar to the calcined MWW precursors (Figure 7).

The above conclusions have also been confirmed from BJH pore size distributions (Figure S3, Supporting Information), where it is observed that the intercalated samples (MWW-BTEB and MWW-BTEB-NH_2) present a distribution centered at 40−50 Å associated to the mesoporosity generated between the layers due to the presence of silyl-aryl groups. On the contary, the calcined precursors do not show mesoporous contribution. On the other hand, the MWW zeolitic materials exhibit the peculiarity that 10 MR sinusoidal channels are present into the layers, being also possible to observe this microporosity in the hybrid samples from Horvath−Kawazoe pore size distributions (see inset of Figure S3, Supporting Information). This fact confirms that the pillarization process with aryl groups does not modify the internal structuration of the individual inorganic layers, and the final hybrid material has a hierarchically structured micromesoporous system.

3.2. Computational Results. Taking into account the structure of the MWW layers and the structural silanol groups present in the ideal layer, we have attempted to model the intercalated MWW-BTEB material by simulating the location and amount of BTEB molecules, and to simulate the differential infrared features between the hybrid MWW-BTEB and MWW conventional zeolites. The computational methodology used is presented in the Supporting Information.

3.2.1. Location and Structure of BTEB in the Pillared MWW-BTEB Material. Each BTEB molecule binds to two MWW layers through condensation with two opposing OH groups located in each of the two MWW layers. Within the hexagonal symmetry of MWW zeolitic precursor each SiOH group is surrounded by 3 neighbor SiOH, with neighbor OH groups separated by 8.2 Å (Figure S4, Supporting Information). BTEB are bulky molecules but a distance of 8.2 Å is enough to allow the location of neighbor BTEB, as shown in Figure 8, based on the results of our lattice energy minimization calculations. The possible ratio of "substituted OH"/"total OH" spans the entire range between 0 and 1, which means that, theoretically, any number between 0 and 8 BTEB molecules can be present in the model of Figure 8. At this point, we can estimate the BTEB content, and the stochiometry of the MWW-BTEB material, based on the following analysis:

The unit cell of MWW zeolitic materials considered has the stoichiometry $Si_{72}O_{146}H_4$, which, structurally, can be expressed as $68 \cdot SiO_2[O_{3/2}-SiOH]_4$, where each silanol group is indicated as a $[O_{3/2}-SiOH]$ unit (see Figure S5,Supporting Information). As a test of the forcefield, this unit cell was optimized, and the resulting structure gave a value of 14.15 Å for the "a" and "b" cell parameters, in good agreement with the experimental value of 14.21 Å[39] for pure silica MWW zeolites.

With the above considerations, a $2 \times 2 \times 1$ unit cell of conventional MWW materials containing two layers and 16 silanol groups (Figure S4, Supporting Information) was considered, whose stoichiometry is indicated in eq 1.

$$272 \cdot SiO_2[O_{3/2}-SiOH]_{16} \quad (1)$$

If we take "2*x*" as the number of silanol groups ("*x*" is the number of silanol groups of each layer), and considering the presence of the pillarizing BTEB molecules into the MWW-BTEB material, the following expression can be written:

$$272 \cdot SiO_2[O_{3/2}-SiOH]_{2x}[O_{3/2}-SiO-BTEB-OSi-O_{3/2}]_y \quad (2)$$

in where $2x + 2y = 16$, since each BTEB molecule replaces two silanol groups, and hence:

$$x + y = 8 \quad (3)$$

Substituting the BTEB molecule by its composition it results:

(39) Camblor, M. A.; Corma, A.; Díaz-Cabañas, M. J.; Baerlocher, Ch. *J. Phys. Chem. B* **1998**, *102*, 44.

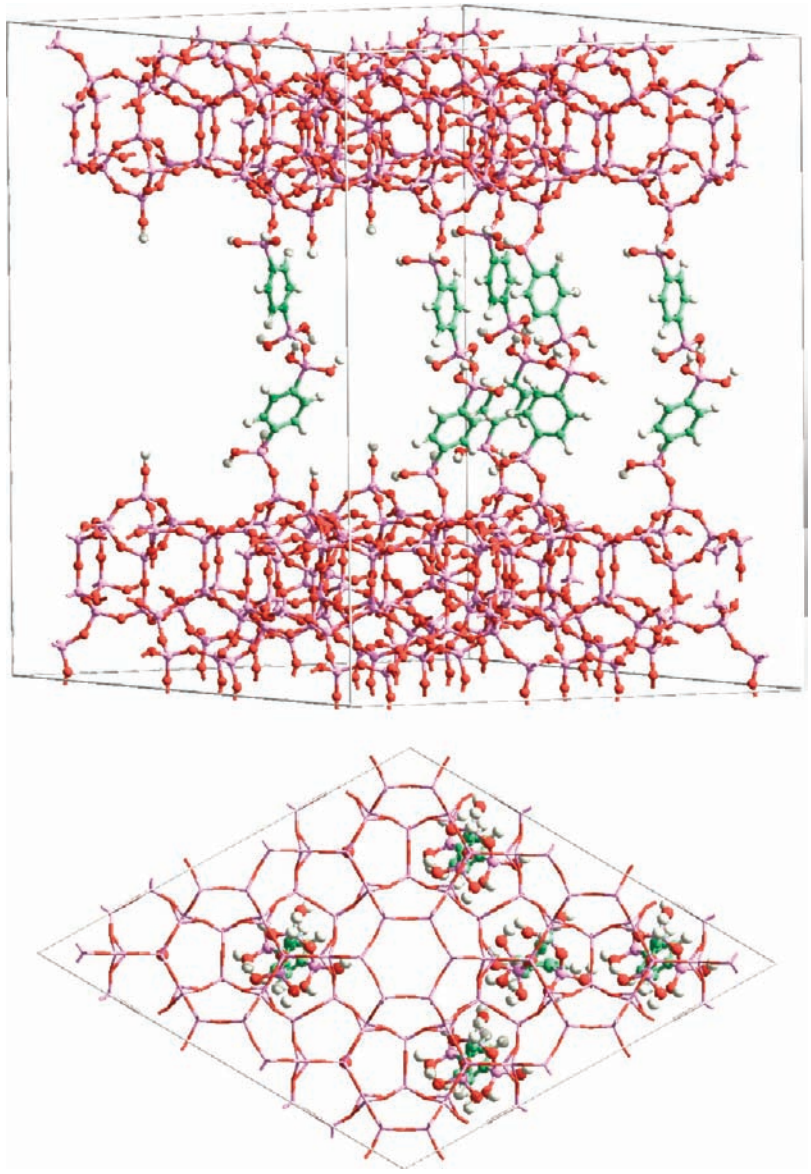

Figure 8. Model of MWW-BTEB hybrid where 5/8 of the silanol groups have reacted to give the interlayer arylic pillar. The resulting organic content (10.7%) is discussed in the text.

$$272 \cdot SiO_2[O_{3/2}-SiOH]_{2x}[O_{3/2}-SiO-(Si_2O_4C_6H_8)O(Si_2O_4C_6H_8)-OSi-O_{3/2}]_y \quad (4)$$

Taking the organic content (o.c.) as the relative weight of the BTEB molecules compared to the total system and using eqs 3 and 4, we have the possibilities shown in Table 3. The chemical analysis described before (Table 1) indicates that the organic content is ∼10 wt %, which is quite similar to the case $y = 5$ (10.7%), and hence the cases $y = 7$, 8 have not been considered in Table 3.

Minimization of the corresponding unit cell ($y = 5$) gives a geometry compatible with the expected chemical bonds and angles near their equilibrium values, this meaning that the full system is reasonably stable (Figure 8). Further analysis of the second derivatives of the energy with respect to the coordinates showed no negative eigenvalues ensuring that the geometry corresponds to a minimum. A detailed structural analysis is available in the Supporting Information. Importantly, the optimized "c" parameter found for this system is 39.8 Å, which is in good agreement with the XRD experimental determination of 40.1 Å (Figure 1).

Table 3. Relation between "*y*", the Number of BTEB Molecules As Indicated in eq 4, and the Organic Content in the MWW-BTEB Material

y	o.c. (%)
1	2.3
2	4.6
3	6.7
4	8.7
5	10.7
6	12.5

3.2.2. Simulation of the Infrared Spectrum and Vibrational Properties of the Intercalated MWW-BTEB Material. A large cluster (Figure 9) has been selected as a representative part of the MWW-BTEB structure. The cluster keeps the interlayer separation obtained from the previous forcefield optimization at 39.8 Å, and it is now fully reoptimized by means of the first principles (electronic) Hartree−Fock method using

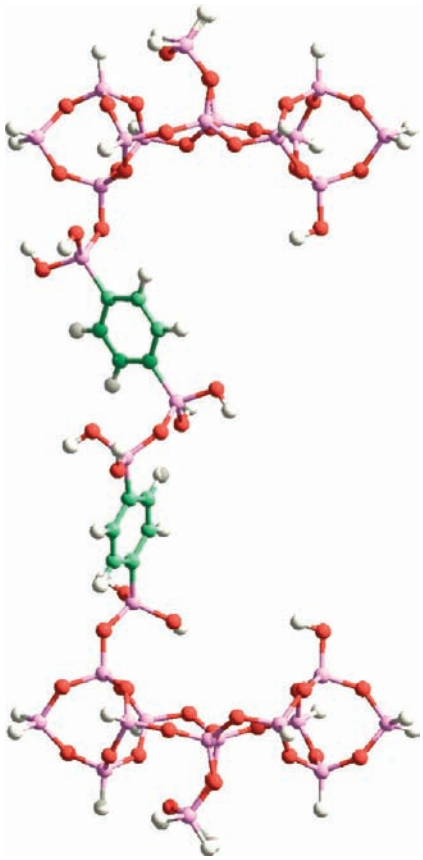

Figure 9. Representative cluster of the MWW-BTEB material containing one BTEB molecule and two silanol groups. The distance between layers corresponds to that which makes the "c" parameter in the optimized unit cell (39.76 Å). This cluster is used for the ab initio Hartree−Fock geometry optimization (final geometry shown) and subsequent vibrational analysis (Figure 10, bottom). An entirely similar cluster without the pillarizing BTEB molecule (containing two additional silanol groups), which corresponds to a model of conventional MWW zeolite, has also been considered for the sake of comparison (vibrational analysis shown in Figure 10, top).

a STO-3G basis set. The normal modes and their intensities are used to calculate the infrared spectrum in Figure 10, which also shows the spectrum of the BTEB-free material (conventional MWW) for the sake of comparison.

The differential features in the IR spectra of MWW-BTEB and MWW are the bands at 1417 cm^{-1} and 3165 cm^{-1}. From the analysis of the eigenvectors of the normal vibrational modes such bands can be assigned to HCC benzene bending (perhaps combined with C−C stretching) and to CH stretching influenced by a nearby OH group, respectively.

Finally, the band at 3676 cm^{-1}, present in both spectra (Figure 10), is due to the OH stretching coming from the silanol groups and the OH groups in BTEB. This explains why this band is more intense in the MWW-BTEB (Figure 10, bottom) than in conventional MWW (Figure 10, top).

The theoretical calculations confirm that the assumptions made on the bases of characterization results are consistent with the fact that a well-structured hybrid organic−inorganic material has been produced, in where zeolitic layers containing microporous channels are the inorganic building blocks, while the organic component is located in between layers forming pillars at regular distance between them generating a 2D mesoporous system.

3.3. Catalytic Activity. The catalytic activity of the hybrid material (MWW-BTEB-NH_2) was studied in a one-pot−two-

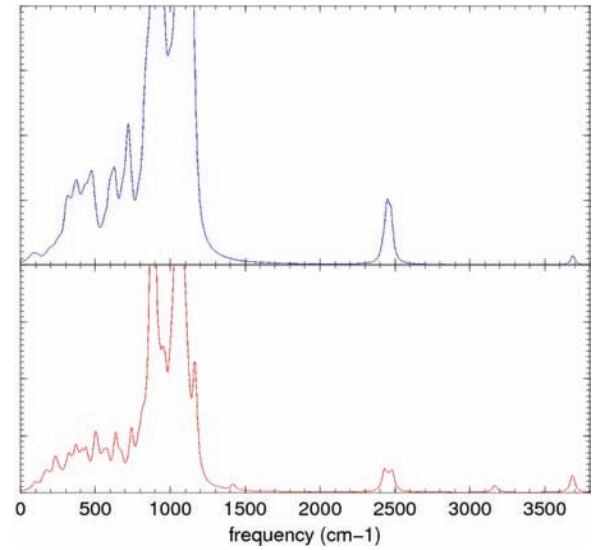

Figure 10. Infrared spectra of the two clusters explained in Figure 9 calculated at the ab initio Hartree−Fock/STO-3G level. Top: MWW zeolite. Bottom: MWW-BTEB hybrid.

Scheme 2. One-Pot Acetal Hydrolysis-Knoevenagel Condensation Cascade Reaction

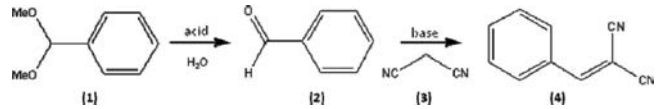

step chemical process that requires acid and base sites, in order to show the catalytic possibilities of the bifunctional organic−inorganic layered material. The cascade reaction studied involved an acetal hydrolysis followed by a Knoevenagel condensation.[40−42] More specifically, benzaldehyde dimethylacetal was hydrolyzed to produce benzaldehyde which reacts with malononitrile to give benzylidene malononitrile (see Scheme 2). The first reaction step requires acid sites which can be supplied by the MWW aluminosilicate layers, while the condensation step involves basic sites which are the amino groups in the arylic molecules forming the mesoporous gallery. The results showed that the tandem reaction was successfully performed, giving the final product (**4**) with a yield of 96% after 7.2 h of reaction time, with a selectivity of 99% (entry 1, Table 4). From Figure 11, it is possible to observe the conversion of the starting dimethylacetal and the formation of the benzaldehyde (**2**) that reacts through the consecutive Knoevenagel condensation with malononitrile to give the final product.

When the consecutive catalytic process is performed with a MWW-BTEB material (the acid counterpart) without amino groups onto the arylic interlayered fragments (entry 2, Table 4), the acid hydrolysis of acetal is carried out (conversion of 51%), but the product of Knoevenagel condensation is produced with a yield of only 11%. This confirms unambiguously that the contribution of acid sites located in the inorganic layers of the hybrid materials to catalyze the Knoevenagel condensation is very small, being this step clearly catalyzed by the basic sites located into the interlayer space in the amino functionalized MWW-BTEB catalyst. Finally, a blank experiment was per-

(40) Margelefsky, E. L.; Zeidan, R. K.; Dufaud, V.; Davis, M. E. *J. Am. Chem. Soc.* **2007**, *129*, 13691.
(41) Bass, J. D.; Katz, A. *Chem. Mater.* **2006**, *18*, 1611.
(42) Katz, A.; Davis, M. E. *Nature* **2000**, *403*, 286.

Table 4. One-Pot Acetal Hydrolysis-Knoevenagel Condensation Cascade Reaction

entry	catalyst[a]	conversion of **1** (%)	yield of **2** (%)	yield of **4** (%)
1	MWW-BTEB-NH_2	99	3	96
2	MWW-BTEB without amino groups	51	40	11
3	blank[b]	−	97	3

[a] Reaction conditions: benzaldehyde dimethylacetal (5.45 mmol), malononitrile (5.24 mmol), H_2O (30 μL, 33 mol %) and layered hybrid catalysts (50 mg), 2 mL of acetonitrile as solvent, 355 K, 7.25 h of reaction time. [b] Knoevenagel reaction: benzaldehyde (5.45 mmol), malononitrile (5.24 mmol), H_2O (30 μL, 33 mol %) and layered hybrid catalyst (50 mg), 2 mL of acetonitrile as solvent, 355 K, 7.25 h.

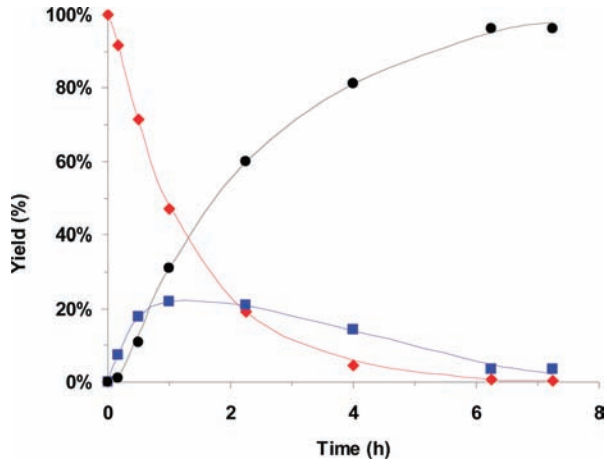

Figure 11. Results of the catalytic activity of the bifunctional layered hybrid material (MWW-BTEB-NH_2) for hydrolysis-aldol cascade reaction. Yields versus reaction time of benzaldehyde dimethylacetal (**1**) (◆), benzaldehyde (**2**) (■) and benzylidene malononitrile (**4**) (●).

formed (entry 3, Table 4). The results show that, under these conditions, the Knoevenagel condensation does not occur (yield of 3% after 7.2 h).

Additionally, catalyst deactivation and reusability was studied by recycling the used hybrid catalyst after each run, after being washed with ethyl acetate. Figure S6 (Supporting Information) shows the yield to benzylidene malononitrile (4) after up to four reuses. It can be observed that the reused catalyst maintains the initial activity, indicating that the bifunctional hybrid zeolitic materials can be of interest as heterogeneous catalyst. The presence of a hierarchical system of micro and mesoporous can be used in further studies to gain additional selectivity features.

We predict that the type of materials designed here can be of interest for preparing multifunctional acid−base redox catalysts, since cations such as Ti, Fe, Sn or Zr can also be introduced in the framework positions of the inorganic building blocks. Furthermore, metal or oxide nanoparticles could also be supported on the inorganic counterpart of the hybrid organic−inorganic materials described here, and in this way, well-defined multifunctional hybrid organic−inorganic robust catalysts could be prepared.

4. Conclusions

4.1 Novel layered zeolitic hybrid organic−inorganic materials have been successfully prepared, with zeolitic layered MWW precursors as inorganic building blocks and arylic bridged silsesquioxanes which are covalently intercalated into the interlayer space as the organic component.

4.2 The resultant material contains a hierarchical system of pores. In the zeolitic counterpart, acid sites are located within the micropores, while in the mesopores formed by intercalation of the organic, basic amino groups have been incorporated on the aryl molecules.

4.3 The bifunctional solids are stable up to 400 °C in air and can show interesting catalytic properties as illustrated by a cascade reaction which involves acetal deprotection and consecutive Knoevenagel condensation catalyzed by accessible acid and basic sites located in the inorganic and organic building components of the hybrid layered materials.

Acknowledgment. We are thankful financial support by Consolider - Ingenio 2010 (MULTICAT project). T.G. is grateful for JAE predoctoral fellowship from CSIC.

Supporting Information Available: Figures S1−S3 show characterization results related with the aluminum content and textural properties (microporous surface area and pore size distribution) exhibited by the MWW hybrid materials; Figures S4 and S5 show the MWW models employed in the computational study, explained by the methodology following in the theoretical section; Figure S6 shows the recyclability of the hybrid catalyst. This material is available free of charge via the Internet at http://pubs.acs.org.

JA106272Z